

Anodic Shaping and Cathode Shape Design

The two fundamental problems in ECM are (i) the prediction of the resultant anode shape when the cathode shape is known, and (ii) the design of the cathode shape to achieve a required anode shape. The second problem is by far the more difficult, and it can be regarded as the primary one of ECM.

Basic approaches for tackling the two problems are of interest. First, analytic solutions are possible, although they have proved to be limited in their applicability. Because of this drawback, the ‘cos θ ’ method for cathode design has been developed; in addition, analogue techniques have been tried, although they have their own limitations. The best means of solution to the problems of shaping in ECM seems to be offered by numerical methods. Even these, however, seldom incorporate effects often encountered in ECM, for instance, those arising from the electrolyte flow. The inclusion of such phenomena in any analysis would render almost intractable the general problem of electrochemical shaping. Indeed, the lack of progress in solving this problem has meant that empirical methods are still widely used in practice.

7.1 Solutions by analysis

As in the previous chapter, three basic equations are used.

(i) Laplace’s equation:

$$\nabla^2 \phi = 0 \quad (7.1)$$

Anodic Shaping and Cathode Shape Design

the solution of which gives the potential ϕ in the electrolyte, particularly at the electrode surfaces.

(ii) Ohm’s law:

$$\mathbf{J} = -\kappa_e \nabla \phi \quad (7.2)$$

where \mathbf{J} , the current density, will be found from the potential from Equation (7.1), κ_e being the electrolyte conductivity.

(iii) Faraday’s law:

$$\dot{r}_a = \left(\frac{A}{z\rho_a F} \right) \mathbf{J} \quad (7.3)$$

in the usual notation, which is used to find the anodic dissolution rate.

Two procedures are known to be available for solving these equations.

7.1.1 A perturbation method [1]

This method has been used to describe electrochemical shaping when the amplitude of shapes on the cathode and anode is small compared with the inter-electrode gap. The small size of the shapes on the electrodes will be shown below to restrict the use of this method to a limited range of shaping problems. Nevertheless, this treatment usefully demonstrates characteristic behaviour encountered in electrochemical shaping; and, moreover, it can be applied to any electrode shape. It is also one of the few treatments which allows the role of overpotentials to be examined. This method obviously has a close resemblance to the main analysis of anodic smoothing in Chapter 6.

In the previous chapter, the anode irregularities were assumed to be periodic, and a Fourier series expansion was used to describe their behaviour. In this chapter, a more general class of electrode shapes (and, in particular, isolated ones) will be taken, and the corresponding analysis will be performed by means of Fourier transforms.

Consider, first, a case where the cathode shape is known, and the resultant shape on the anode is to be found. Suppose the cathode shape is given by the Fourier integral

$$y_c = \epsilon(0) \int_{-\infty}^{\infty} b(k) e^{ikx} dk \quad (7.4)$$

which represents a small deviation from $y_c = 0$; i.e. $|y_c|/p \ll 1$, where p is the average inter-electrode gap, and $\epsilon(0)$ is the size of irregularity on the electrode surface. Suppose further that the anode is initially plane. (This is not essential to the argument, but simplifies the algebra). After a time t , the anode shape may be described by

$$y_a = p + \epsilon(0) \int_{-\infty}^{\infty} a(k,t) e^{ikx} dk \quad (7.5)$$

The shapes on both anode and cathode will influence the inter-electrode potential which, it is assumed, may be written as a first-order perturbation to the potential between two plane parallel electrodes:

$$\phi = \phi_0 + \frac{\epsilon(0)}{p} \phi_1$$

where ϕ_0 satisfies the boundary conditions $\phi_0 = 0$ on $y = 0$, $\phi_0 = V$ on $y = p$, and ϕ_1 satisfies

$$\begin{aligned} \phi_0 + \frac{\epsilon(0)}{p} \phi_1 &= 0 && \text{on } y = y_c \\ \phi_0 + \frac{\epsilon(0)}{p} \phi_1 &= V && \text{on } y = y_a \end{aligned} \quad (7.6)$$

By procedures similar to those in Chapter 6, an expression can be obtained for the potential:

$$\phi = \frac{V}{p} - V \frac{\epsilon(0)}{p} \int_{-\infty}^{\infty} e^{ikx} \frac{a \sinh ky + b \sinh k(p-y)}{\sinh kp} dk$$

for the rate of change of gap,

$$\frac{dp}{dt} = \frac{MV}{p} - f$$

and for the time-dependence of the Fourier coefficients,

$$\frac{\partial a}{\partial t} = - \frac{M V k}{p} (a \coth kp - b \operatorname{cosech} kp)$$

For constant p , the above equation can be solved to show that the amplitude of any frequency component on the anode tends to the limiting value

$$a(k) = b(k) \operatorname{sech} kp \quad (7.7)$$

as $t \rightarrow \infty$. For $a(k,0) = 0$ (initially smooth anode), it is also pointed out that components with large $|k|$ will have little effect on the profile produced on the anode. The range of possible anode shapes which may be predicted by this method of analysis is therefore restricted. A fuller discussion of these limitations is given elsewhere [1].

When this theory is extended to cover cathode design, further stringent restrictions are imposed. Indeed, the usefulness of this theory for studies of cathode design becomes exceedingly limited. The theory, however, does indicate the approaches required for analytic solutions of the shaping problem in ECM. Moreover, it emphasises the difficulty of the problem.

One further result from that work is of interest: the analysis can be extended to include the effects of overpotential. For an arbitrary current density-dependent overpotential at the cathode only, the limiting amplitude on the anode is shown to be modified to

$$a(k) = b(k) \frac{\operatorname{cosech} kp}{\coth kp + (\mu/\sigma)kp} \quad (7.8)$$

where μ/σ ($= \beta \kappa_e/p$), the dimensionless parameter for the cathode overpotential, previously introduced in Chapter 6, has again been used. Clearly, the limiting amplitude has been multiplied by a factor $\coth kp / [\coth kp + (\mu/\sigma)kp]$, and the profile machined on the anode becomes 'blurred'.

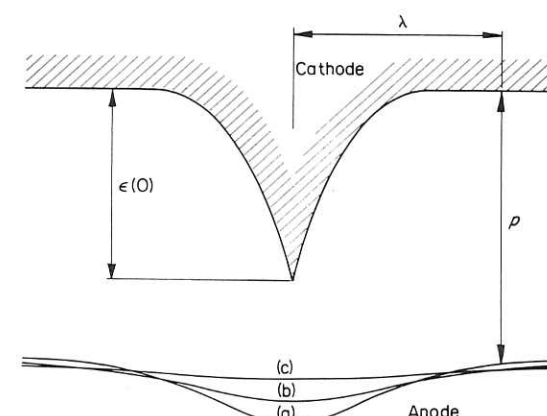


Fig. 7.1 Shape produced on anode by cusp shaped cathode. Shape (a), without overpotential; shapes (b) and (c), with cathode overpotential; $\lambda = 1$ mm; $p = 0.5$ mm; vertical scale magnified twenty times (after Fitz-Gerald et al. [1])

Overpotentials only at the anode can be shown to have no effect on the limiting amplitude on the anode shape. But overpotentials at either electrode are shown to increase the time of ECM necessary to achieve the limiting amplitude on the anode.

Example

Figure 7.1 indicates the shape produced on the anode by an isolated cusp on the cathode. Curve (a) represents the anode profile, when overpotentials are not considered. Curves (b) and (c) demonstrate the ‘blurring’ of this profile by overpotentials at the cathode only. The amount of this overpotential is defined by the quantity μ/σ ($= \beta\kappa_e/p$): $\mu/\sigma = 1$ [curve (b)]; $\mu/\sigma = 10$ [curve (c)].

7.1.2 A complex variable method

Methods of solutions of Laplace’s equation with specified boundary conditions by this method are well known, and can be found in any of the standard textbooks. In brief, the basis of any such approach is as follows.

Suppose a solution is sought for the two-dimensional Laplace’s equation:

$$\frac{\partial^2 \phi}{\partial x^2} + \frac{\partial^2 \phi}{\partial y^2} = 0$$

To solve this equation, we put $z = x + iy$, where $i = \sqrt{-1}$. Next, consider any function of z , which is written

$$\omega = f(z) = f(x + iy) = \phi(x, y) + i\psi(x, y) \quad (7.9)$$

That is, ϕ and ψ are real and imaginary parts of $f(z)$.

By partial differentiation of $\omega = f(x + iy)$:

$$\frac{\partial^2 \omega}{\partial x^2} + \frac{\partial^2 \omega}{\partial y^2} = 0 \quad (7.10)$$

Separation of the real and imaginary parts yields

$$\nabla^2 \phi = 0 \quad \text{and} \quad \nabla^2 \psi = 0 \quad (7.11)$$

Hence ϕ and ψ are possible potential functions satisfying Laplace’s equation. Note that, on partial differentiation of Equation (7.9),

$$\frac{\partial \omega}{\partial y} = if'(z) = i\frac{\partial \omega}{\partial x}$$

That is,

$$\frac{\partial \phi}{\partial x} = \frac{\partial \psi}{\partial y} = \text{real part of } f'(z) \quad (7.12)$$

$$\frac{\partial \psi}{\partial x} = -\frac{\partial \phi}{\partial y} = \text{imaginary part of } f'(z) \quad (7.13)$$

Solutions to Laplace’s equation can now be obtained either directly from known functions, e.g. $f(z) = z^3$, the boundary conditions being known, so that equipotential lines can be defined, or by means of the method of electrical images, or by conformal mapping. The last mentioned approach is most effective for ECM problems. Its principle consists of the transformation of one problem into another which is tractable.

Thus, the transformation $\xi = f(z)$ transforms a point z in the (x, y) -plane into a point $\xi = \xi + i\eta$ in the (ξ, η) -plane. Since $d\xi = f'(z)dz$, $|d\xi| = |f'(z)| |dz|$, $\arg d\xi = \arg f'(z) + \arg dz$.

Two points can now be made: (i) in the vicinity of the point $z = z_0$, where $\xi = \xi_0 = f(z_0)$, all distances in the ξ -plane are $|f'(z_0)|$ times greater than the corresponding distances in the z -plane; (ii) small arcs are turned through an angle $\arg f'(z_0)$. Thus a small element of area in the z -plane becomes an element in the ξ -plane. The latter element has the same shape, but has dimensions magnified by $|f'(z_0)|$, the element being rotated through an angle $\arg f'(z_0)$.

Thus, if a function $\phi(x, y)$ can be expressed in terms of ξ and η , $\Phi(\xi, \eta)$, by the transformation $\xi = f(z)$ then

$$\frac{\partial^2 \Phi}{\partial \xi^2} + \frac{\partial^2 \Phi}{\partial \eta^2} = \frac{1}{|d\xi|^2} \left(\frac{\partial^2 \phi}{\partial x^2} + \frac{\partial^2 \phi}{\partial y^2} \right) \quad (7.14)$$

Suppose

$$\frac{\partial^2 \phi}{\partial x^2} + \frac{\partial^2 \phi}{\partial y^2} = 0$$

Then

$$\frac{\partial^2 \Phi}{\partial \xi^2} + \frac{\partial^2 \Phi}{\partial \eta^2} = 0$$

so that Φ is a potential function in the (ξ, η) -plane.

In the application of complex variable techniques to the shaping problem in ECM, the three equations (7.1), (7.2), and (7.3) are again used. As usual, any analysis is eased by the assumption of steady-state machining conditions, and by the exclusion of the effects of electrolyte flow and overpotentials.

For these conditions, the potential boundary conditions are given by Equations (6.4) and (6.5):

$$\phi = 0 \quad \text{on the cathode}$$

$$\phi = V \quad \text{on the anode}$$

Since steady-state ECM is taking place, a further condition on the anode is that the normal dissolution rate of the anode surface equals the cathode feed-rate in that direction. That is,

$$\kappa_e \left(\frac{\partial \phi}{\partial n} \right) = f \cos \theta \quad (7.15)$$

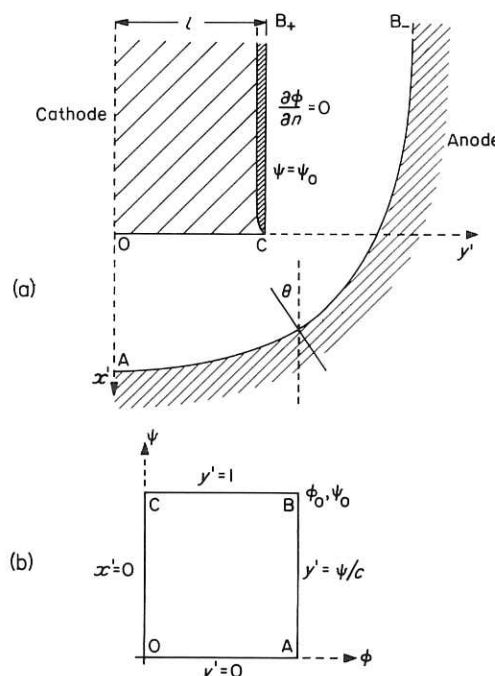


Fig. 7.2 (a) Configuration for a plane-faced cathode tool with insulation; (b) boundary conditions in the ω -plane (after Collett et al. [2])

where $(\partial \phi / \partial n)$ is the normal component of the electric field at the anode surface, f is the cathode feed-rate (in the vertical direction), and θ is the angle between the normal to the anode boundary and the direction of cathode movement.

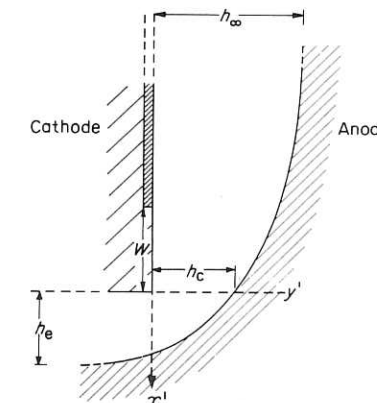


Fig. 7.3 Straight-sided cathode with finite uninsulated land width at base and insulated upper length; $W = 1.86h_e$; $h_\infty = 3.36h_e$ (after Hewson-Browne [3])

These approaches have been used to find the equilibrium anode shapes resulting from two particular cathode shapes: (i) a plane-faced cathode with complete insulation on its side walls (Fig. 7.2), and (ii) a partly uninsulated, straight-sided cathode (Fig. 7.3) [2, 3].

From the methods of complex variables, the electric field in the electrolyte between the electrodes is

$$\mathbf{E} = (E_x, E_y)$$

and

$$\bar{E} = E_x - iE_y = \frac{d\omega(z)}{dz}$$

where $z = x + iy$, and $\omega = \phi + i\psi$.

The boundary conditions (6.4) and (6.5) and (7.15) apply. On the insulated surfaces of the cathode, the normal component of the electric field is zero, so that

$$\psi = \text{constant} \quad (7.16)$$

on these surfaces.

Another form of Equation (7.15) is useful:

$$\frac{\partial \phi}{\partial n} = \tau \cos \theta \quad (7.17)$$

where τ is a constant, obtained from the machining parameters.

If s is the arc length measured along the anode boundary S in the direction of increasing y' ,

$$\cos \theta = \frac{\partial y'}{\partial s}$$

and

$$\frac{\partial \phi}{\partial n} = \frac{\partial \psi}{\partial s}$$

Thus, on integration the boundary condition (7.17) becomes

$$\psi = \tau y' \quad (7.18)$$

Since the electrode configuration [Fig. 7.2(a)] is symmetrical about the x' -axis, and since, from Equation (7.18), $\psi = 0$ at A, we have that $\psi = 0$ on OA.*

Also, from Equation (7.16),

$$\psi = \psi_0 \text{ on } B_+C$$

Thus, only the region OABCD needs consideration, and that region is now mapped onto the ω -plane. The boundary conditions in the ω -plane are shown in Fig. 7.2(b).

A solution for ω of the form

$$z = \frac{\omega}{\tau} + \sum_{n=0}^{\infty} a_n \sin \left[(2n+1) \frac{\pi \omega}{2V} \right] \quad (7.19)$$

is now sought so that conditions on OA, AB, and CO are satisfied.

Here a_n are real constants.

When this analysis is carried out, the configuration of electrodes can be shown to be specified by the parameters V , τ , and l , where $2l$ is the width of the cathode. When some typical values, $V/\tau = 1.014l$, $h_e = 0.899l$, and $h_\infty = 1.006l$, where h_∞ is the total overcut at B_+B_- , are used to describe the limiting anode surface, one further result of

* In the study on which this treatment is based [2] the x and y axes are interchanged from the convention adopted elsewhere in this chapter. To maintain the sequence of argument, but at the same time to avoid confusion, the symbols x' and y' are used here; so that elsewhere $x = y'$ and $y = x'$.

interest can be obtained. It predicts that the overcut at the corner C of the cathode is related to the equilibrium gap by the relation

$$\frac{\text{overcut at corner C}}{\text{equilibrium gap (OA)}} \approx 0.731 \quad (7.20)$$

For a cathode without insulation along the side BC, further analysis by mapping yields that

$$\frac{\text{overcut at corner C}}{\text{equilibrium gap (OA)}} = 1.159 \quad (7.21)$$

This method of analysis has been extended to cover a wider class of cathode tools in which the straight-sided cathode has a finite un-insulated land width W at its base as well as an insulated portion [3] (see Fig. 7.3).

Two consecutive mappings are used to show that the variation of the total overcut h_∞ with equilibrium gap is given by

$$\frac{h_\infty}{h_e} = 1 + \frac{1}{4} \left(\frac{3\pi W}{h_e} \right)^{2/3} + \dots \quad (7.22)$$

for $W \ll h_e$, and

$$\frac{h_\infty}{h_e} \approx \left(\frac{2W}{h_e} \right)^{1/2} + \frac{2}{\pi} \log 2 + \dots \quad (7.23)$$

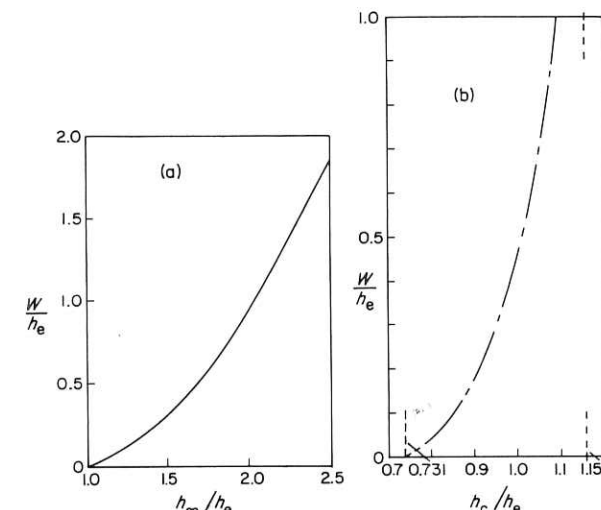


Fig. 7.4 Land width W as a function of (a) total overcut h_∞ , and (b) overcut at the corner of the cathode, h_c (after Hewson-Browne [3]).

for $W \gg h_e$. The variation in the total overcut h_∞ with the land width W is shown in Fig. 7.4(a), whilst the dependence of the overcut at the corner on land width is given in Fig. 7.4(b).

In practice, the overcut in electrochemical hole-drilling can be reduced, and the accuracy of drilling improved, by the use of a passivating electrolyte, which yields current efficiencies which are low and high, respectively, at low and high current densities. The former condition is achieved in the region of the side gap, whilst high current efficiencies at the high current densities are obtained along the main, front machining gap.

7.2 Solution by the 'cos θ ' method

The limited availability and usefulness of analytic solutions to the shaping problem have meant a search for alternative methods which are simpler to handle and which are useful in tackling a range of practical problems. Accordingly, the so-called 'cos θ ' method has received considerable attention [4–6]. Again, this procedure is based on steady-state machining conditions, and it excludes consideration of electrolyte flow and overpotential effects. Its main features can be explained with reference to Fig. 7.5.

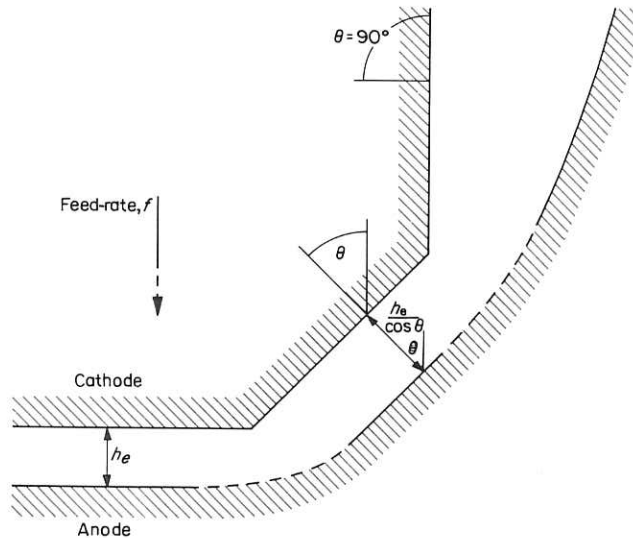


Fig. 7.5 Principle of the 'cos θ ' method (after Tipton [4])

Consider a cathode tool which consists of several planar sections inclined at different angles, θ . The equilibrium gap between any section of the cathode surface and that corresponding surface of the anode which is parallel to it is $h_e/\cos \theta$. As before, θ is measured between the normal to the anode surface and the direction of cathode feed. The 'cos θ ' method of cathode design can be applied to electrode regions where the electric field can be assumed to be normal to the surfaces of the electrodes. It cannot, of course, be applied to regions corresponding to discontinuities at the cathode surface, and where the angle θ is great ($\approx 90^\circ$); that is, its application is limited to regions where the local radii of curvature of the anode and cathode surfaces are large compared with the equilibrium gap.

The following parametric equations have proved useful for calculating the cathode shape necessary for a required anode shape [4].

Suppose that the anode shape is given by

$$y = f(x) \quad (7.24)$$

Any point, $A(x, y)$, say, on the anode surface then corresponds to an

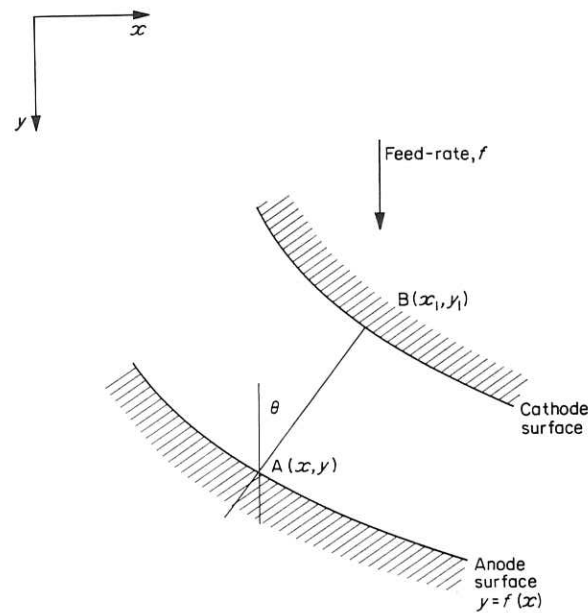


Fig. 7.6 Cathode design by 'cos θ ' method

equivalent point B(x_1, y_1) on the cathode, the gap width between A and B being $h_e/\cos \theta$ (Fig. 7.6). We have

$$\begin{aligned} y - y_1 &= AB \cos \theta \\ &= h_e \end{aligned} \quad (7.25)$$

and

$$\begin{aligned} x_1 - x &= AB \sin \theta \\ &= h_e \tan \theta \\ &= h_e \left(\frac{dy}{dx} \right) \end{aligned} \quad (7.26)$$

Suppose, now, that a general expression for the anode surface is

$$y = a + bx + cx^2 \quad (7.27)$$

Use of the above equations then yields

$$y_1 + h_e = a + bx_1 + cx_1^2 - bh_e \frac{dy}{dx} - 2cx_1 h_e \frac{dy}{dx} + ch_e^2 \left(\frac{dy}{dx} \right)^2 \quad (7.28)$$

Now from Equations (7.26) and (7.27),

$$\frac{dy}{dx} = \frac{b + 2cx_1}{1 + 2ch_e} \quad (7.29)$$

and substitution of Equation (7.29) into (7.28) gives

$$y_1 = a + bx_1 + cx_1^2 - h_e - h_e \left[\frac{(b + 2cx_1)^2}{1 + 2ch_e} \right] \quad (7.30)$$

in which terms of order $h_e^2(dy/dx)^2$ have been assumed negligible.

In Equation (7.30) the first four terms still describe the anode surface, but indicate its displacement through a distance h_e . The final term includes the correction for the curvature of the anode.

The graphical and analytic means of predicting electrode shapes by the 'cos θ ' method have largely been replaced by computational techniques.

7.3 Analogue methods of solution

Analogue methods for solving Laplace's equation are well known, and their application to the ECM problem of anode shaping has been the subject of several investigations. In all these studies, the same

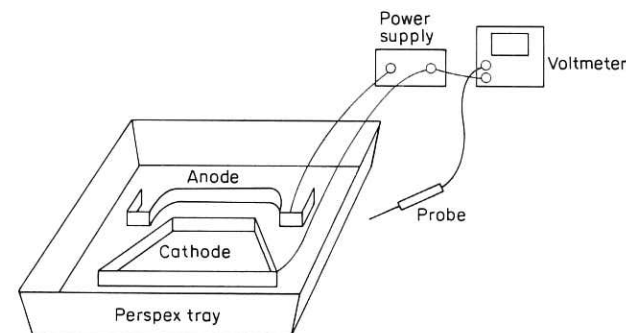


Fig. 7.7 Equipment for electrolytic tank analogue

principles are used. One electrode boundary shape is fixed and known (for example, the cathode). The potential conditions between the electrodes and at their boundaries are also known. The other electrode shape is now sought so that certain boundary conditions are met. These boundary conditions, as usual, are

$$\phi = 0 \text{ on the cathode}$$

$$\phi = V \text{ constant on the anode}$$

$$\frac{\partial \phi}{\partial n} = \text{constant at the anode}$$

7.3.1 'Electrolytic tank' analogue method

The basic equipment consists of a shallow perspex tray, filled with electrolyte (e.g. copper sulphate solution), and thin metal strips (e.g. copper) which can be clamped in position in the tray. The strips represent the anode and cathode boundaries. Insulated boundaries are likewise represented by perspex strips. A small voltage (1 to 3 V) is applied between the electrodes from a stabilised power supply. It is measured with a high input impedance voltmeter connected to a probe, so prepared that potential differences between the head of the probe and the electrode boundary are reduced as much as possible (see Fig. 7.7).

Suppose, for example, that the cathode shape is fixed and the anode shape is to be found. Enlarged scale drawings of the shape of the known boundary and the *probable* equilibrium shape of the anode are then prepared, preferably on graph paper. On the anode boundary a control point is fixed from which a line normal to the

known cathode boundary can be drawn. At points along the anode boundary, the ratios are noted of the normal potential gradients relative to the fixed control point. (The ratios, of course, are the cosines of the angles of inclination.)

The drawing is now placed under the tray, and the metal and perspex strips are clamped in positions corresponding to those of the drawing. A suitable potential difference is applied between the electrodes. The ratios of the experimentally derived normal potential gradients are then compared with those obtained graphically. If the ratios agree, then the boundary shape has been found. If they are not similar, the positions of the shapes must be altered on the graph paper, and the procedure repeated until the ratios are similar.

The method is applicable to either cathode or anode shape. The procedure, of course, is simplified if the anode shape is fixed and the cathode shape is to be found. In that case, no alteration of electrode shape on the graph paper is required; the cathode shape need only be altered on the electrolyte tray until its position yields satisfactory agreement between the above ratios.

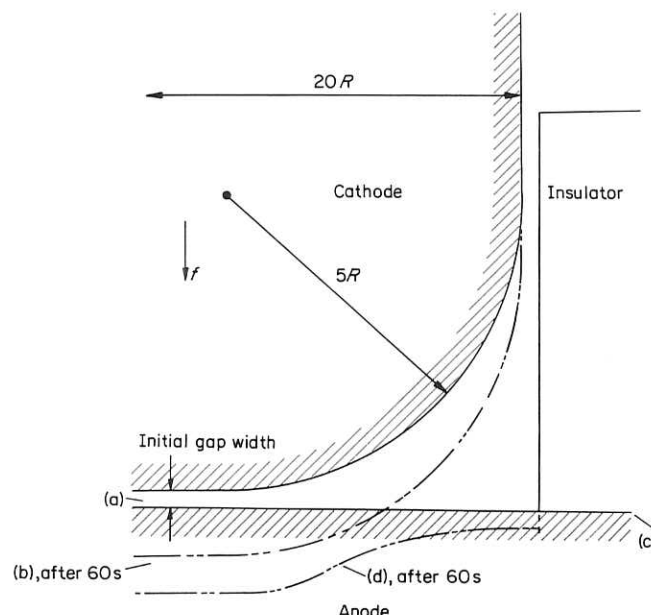


Fig. 7.8 Initial and intermediate positions of cathode [(a) and (b)] and anode [(c) and (d)] (after Kawafune et al. [7])

The same procedures can also be used to find intermediate electrode shapes during the machining time taken to achieve equilibrium conditions. Figure 7.8 shows results from one investigation in which the cathode shape was fixed and the anode was initially flat. The

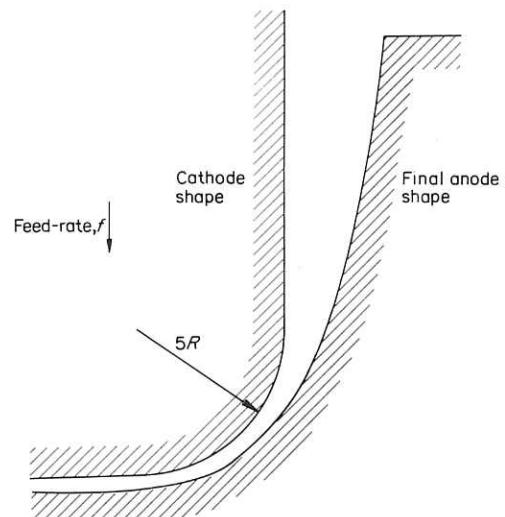


Fig. 7.9 Final anode shape predicted by electrolytic tank analogue (after Kawafune et al. [7])

position occupied by the cathode after a machining time of 60 s is also shown (the cathode feed-rate was 0.002 mm/s.) The resultant anode shape, corresponding to this new position of the cathode, was obtained by the electrolytic tank method, and is also indicated. Repeated applications of the technique yielded the final equilibrium anode shape given in Fig. 7.9. Good agreement was found between the equilibrium anode shape predicted by this method and the form achieved under ECM conditions.

7.3.2 Conducting paper analogue method

The conducting paper method is similar to that of the electrolyte tank, except that the cathode and anode shapes are represented by boundaries outlined in conducting paint on conducting paper. A stabilised variable d.c. power supply is used to supply constant current to the paper, and a voltmeter is used to measure the voltage differences between two probes positioned at appropriate places on

the paper. As before, one boundary, the cathode, say, is fixed and the possible shape of the other boundary (the anode) is prepared (Fig. 7.10). The anode shape is also usually sectioned so that the local current density can be measured along it. To simulate the

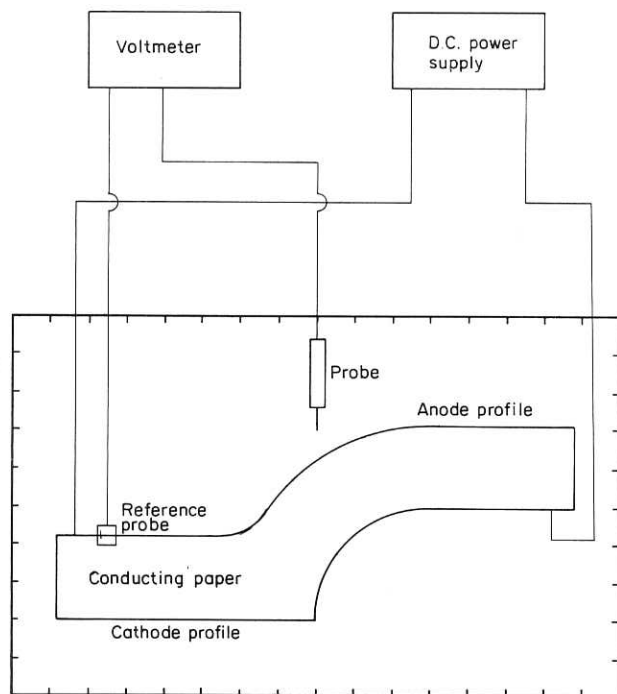


Fig. 7.10 Apparatus for conducting paper analogue

dynamic conditions of ECM, the position of the anode boundary must next be moved through a short distance which corresponds to the change in position after a short time interval, determined by the local ECM conditions (the metal dissolution rate, and hence the current density, and the cathode feed-rate). Such movement can only really be represented by the preparation of a fresh piece of conducting paper for each time interval. Since this procedure is not particularly practical, an alternative device is recommended [8].

Because of the direct ohmic relationship between current and voltage, current distribution lines can be assumed to obey Laplace's equation in the same way as potential lines. Thus the direct analogue, in which potential is constant along the cathode and anode boundaries,

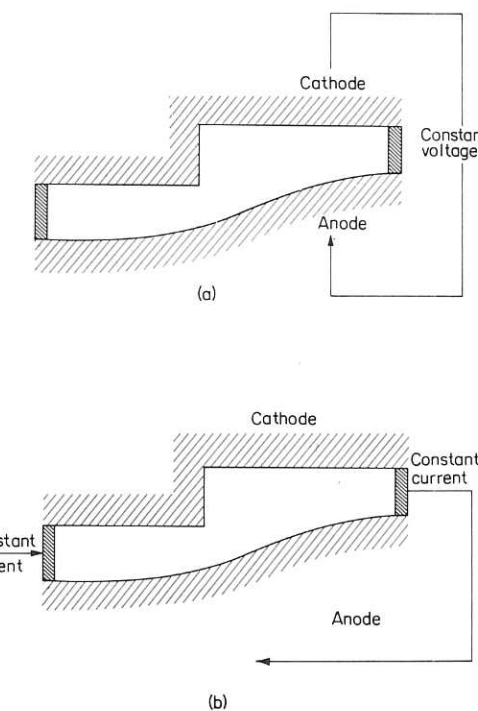


Fig. 7.11 Conducting paper method: (a) direct analogue; (b) 'inverted' analogue (after Tipton [8])

can be replaced by an 'inverse' analogue, in which a constant current is passed through the electrodes painted along the current flow lines (see Fig. 7.11).

The current density J is now represented by the potential gradient $\partial\phi/\partial s$ along the cut edge of the conducting paper, which edge represents the anode surface. This potential gradient is measured from the two probes placed a short distance apart on the edge of the paper.

Consider now Fig. 7.12 which shows conditions at the anode boundary. The vertical vector f represents the feed-rate of the cathode towards the anode. The vector, $\kappa_e(\partial\phi/\partial s)$, which is normal to the anode surface, represents the machining rate and is proportional to the voltage gradient at A. If these velocities are assumed to be constant over time δt , the distances corresponding to these vectors are respectively $f\delta t$ and $(\partial\phi/\partial s)\delta t$. After time δt , the machining causes point A to be transformed to point B. The new anode surface

after time δt is now determined by a series of points such as B. The conducting paper is next cut through these points to obtain the new surface. The above procedure is then repeated until no further

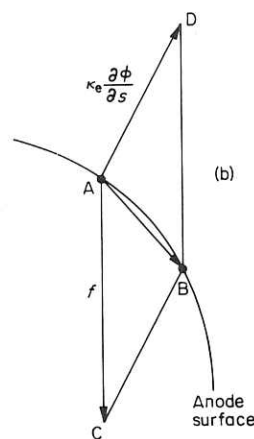
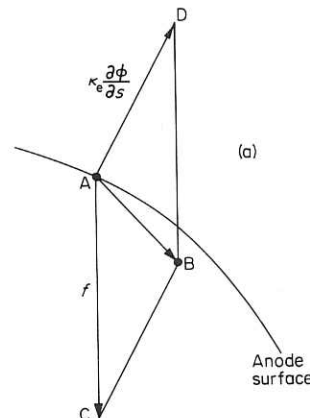


Fig. 7.12 Inverted analogue method: conditions at anode boundary (after Tipton [8])

change in the anode shape is obtained. This final shape is the equilibrium one. Figure 7.13 shows equilibrium anode shapes, predicted by this method, for a stepped cathode with different step sizes [8].

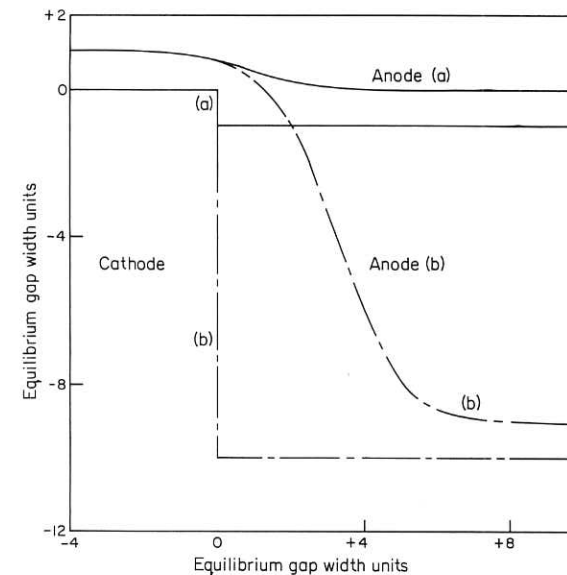


Fig. 7.13 Anode shapes formed with a cathode with step sizes of (a) 1 equilibrium gap width, (b) 10 gap widths (after Tipton [8])

Both analogue methods are tedious to use. In any case, solutions to the field equations for ECM are more easily obtained by means of a digital computer. This approach is discussed in the next section.

7.4 Numerical methods of solution

Numerical methods for solving the shaping problem have the same basis as analogue methods. Suppose that the cathode shape is known and that the anode shape is to be found. An initial, approximate shape, close to the eventual form, for the anode is again chosen, and solutions are sought for the configuration defined by the two electrode shapes and two side walls. Its solution gives the potential at any point between the two electrodes and particularly at the anode. From Ohm's and Faraday's laws the change in shape of the anode boundary, after a small increment of time, can now be found. For these new positions of both electrodes (since the cathode also moves through a distance in the small time interval) Laplace's equation must again be solved. This procedure is repeated until no further appreciable change occurs in the anode shape. The main features of the application to ECM of the well known numerical

and computational techniques [9] for tackling this class of problem are now outlined [5, 6, 10].

7.4.1 Basic method

Numerical solutions to the problem require specification of the coordinates of both the cathode and proposed anode shapes. These coordinates can be defined in terms of an equi-spaced rectangular

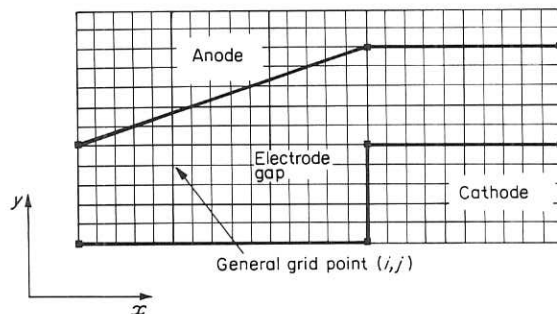


Fig. 7.14 Mesh of grid points defining cathode and anode shapes in terms of coordinates (i,j)

mesh containing a set of grid points of general coordinates (i,j) (Fig. 7.14). A suitable scale, in terms of the mesh spacings, is now chosen for the initial cathode and anode shapes. The size of the scale used depends on the size of computer store available. In turn, the selected scale sets a limit on the electrode dimensions which can be treated. If, as has been recommended [10], five mesh spaces per equilibrium gap unit provide reasonably accurate solutions, then a computer store with, say, 8000 locations limits the mesh area to 320 equivalent units (in terms of the equilibrium gap). That is, the linear dimensions of the electrodes are about 20 equilibrium gap units. Thus for a gap of 0.5 mm this distance is 10 mm.

By this procedure, equipotential boundary lines are obtained which define the electrode forms as well as the electrode gap region in which Laplace's equation is to be solved. (Note: accurate solution to Laplace's equation also requires that the ends of these lines should be terminated in regions where lines of current flow are known, for example, along a plane region of the cathode, or along a line of symmetry parallel to the direction of cathode movement.)

With each grid point is associated some value of the potential within the electrode gap. In addition, the potential values at the grid points on the cathode boundary are made zero, and the values on the anode boundary are set to some large value (e.g. 10 000).

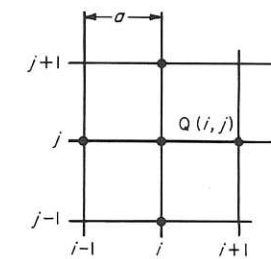


Fig. 7.15 Development of finite-difference method: mesh of side a , with general point $Q(i,j)$

This same value is applied to the bulk anode within the boundary, so that, as the anode is machined, its fresh boundary takes on the same potential value. Those potential values at grid points within the gap are obtained by linear interpolation along the vertical grid lines between anode and cathode. These values at the grid points must now be progressively adjusted until they satisfy a finite-difference equation corresponding to Laplace's equation in the region between the boundaries.

This method can be explained from Fig. 7.15, which represents a square mesh of side a .

The finite-difference equation corresponding to Laplace's equation is

$$\frac{\delta^2 \phi}{\delta x^2} + \frac{\delta^2 \phi}{\delta y^2} = 0 \quad (7.31)$$

in which, given that

$$\begin{aligned} \frac{\delta \phi}{\delta x} &= \frac{\phi(i+1,j) - \phi(i,j)}{a} \\ &= \frac{\phi(i,j) - \phi(i-1,j)}{a} \end{aligned} \quad (7.32)$$

it can be shown that to order (a^2)

$$\begin{aligned}\frac{\delta^2 \phi}{\delta x^2} &= \frac{\phi(i+1,j) - \phi(i,j)}{a} - \frac{\phi(i,j) - \phi(i-1,j)}{a} \\ &= \frac{\phi(i+1,j) - 2\phi(i,j) + \phi(i-1,j)}{a^2} \quad (7.33)\end{aligned}$$

$$\frac{\delta^2 \phi}{\delta y^2} = \frac{\phi(i,j+1) - 2\phi(i,j) + \phi(i,j-1)}{a^2} \quad (7.34)$$

Therefore, the above equation becomes

$$\phi(i+1,j) - 4\phi(i,j) + \phi(i-1,j) + \phi(i,j+1) + \phi(i,j-1) = 0 \quad (7.35)$$

That is, at any point (i,j) in Fig. 7.15, the potential is equal to the average of the potentials at the four neighbouring points.

Next, consider the electrode boundaries, where the potentials are constant. The points on those boundaries do not necessarily lie exactly on mesh points. This means that, for a mesh point adjacent to the boundary, neighbouring points might not have arms of equal length. Accordingly, in the analysis which led up to Equation (7.35) quantities which include the length of the arm (formerly a^2 , a constant) now cannot be cancelled out. For such cases, the above equation clearly cannot be used in its present form.

For instance, suppose that the line PR in Fig. 7.16 defines part of an electrode boundary. Whereas, before, the potential could be easily relaxed at the grid point Q, the adjacent points do not now form a regular array for the same operation to be carried out. In this event, it is customary to relax the potential at, say, point S

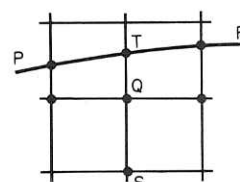


Fig. 7.16 Section of electrode boundary, PTR; long arm ST; potential at Q found by linear interpolation

which has one long arm ST, and then to set the potential at point Q by linear interpolation.

The method of solution now is to adjust repeatedly the potential at each mesh point within the boundaries to a value which is the mean of its four neighbouring points. Eventually, the potential values should approach the correct amounts. During each run, an indication of the deviation of the potential from its correct value at any point can be found from the 'residual' value. This device can be explained from the modified form of Equation (7.35):

$$\phi(i+1,j) - 4\phi(i,j) + \phi(i-1,j) + \phi(i,j+1) + \phi(i,j-1) = R \quad (7.36)$$

where R is the residual, the amount by which the right-hand side of Equation (7.36) differs from zero.

If the potential at any point (i,j) is made the mean of the four neighbouring points, R is zero, or 'relaxed'. In other words, a quantity ($= R/4$) is added to $\phi(i,j)$. The maximum value of the residual gives a measure of the departure of the particular solution from the correct one. The general solution is achieved when the residual becomes smaller than a specified amount. Methods for carrying out this procedure are available elsewhere [6, 9].

The solution so found for these two positions of the electrodes is now used to calculate the normal derivatives of ϕ at the anode, and the anode boundary is now moved by an amount specified by the direction of cathode feed and by the local rate of metal removal. The values of potential previously found for each mesh point now form the initial values for the new solution which is to be found for the fresh position of the boundaries. This procedure is repeated until the changes in the anode boundary become less than the specified amount. This final boundary is the required equilibrium anode shape.

The above procedures can, of course, be used to predict a cathode tool shape for an anode shape which has been specified. But, now the appropriate data specify the known equilibrium anode shape and the probable cathode shape. The relaxation procedure established above is now employed to find the extent by which the normal current density values at the anode have departed from their constant, equilibrium values. Dependent upon the amount of these departures, the cathode boundary is moved, and the relaxation procedure repeated, until the boundary conditions are satisfied. This procedure, however, is by no means easy [6].

7.4.2 Practical considerations

In the application of numerical methods, some useful guide-lines have emerged; the machining conditions for the particular metal-electrolyte combination must be studied to provide data on the process variables, for instance the equilibrium gap width and the cathode feed-rate. Experiments of this sort will also indicate the extent of effects due to electrolyte flow, etc., although such effects have not been included in the analysis. Care must also be taken to ensure that the anode workpiece carries sufficient stock to allow the equilibrium shape to be formed to sufficient tolerance.

7.4.3 Example of numerical methods

Computer solutions to the shaping problem for a variety of fixed cathode shapes have been prepared by Lawrence [6]. Figure 7.17 shows the numerically predicted equilibrium anode profile produced by a semicircular cathode. The figure also shows the profile found by experiment. The upper numbers along the anode boundary represent a non-dimensionalised form of the measured normal voltage gradient; in comparison, the lower numbers show the voltage gradient calculated from the slope of the boundary.

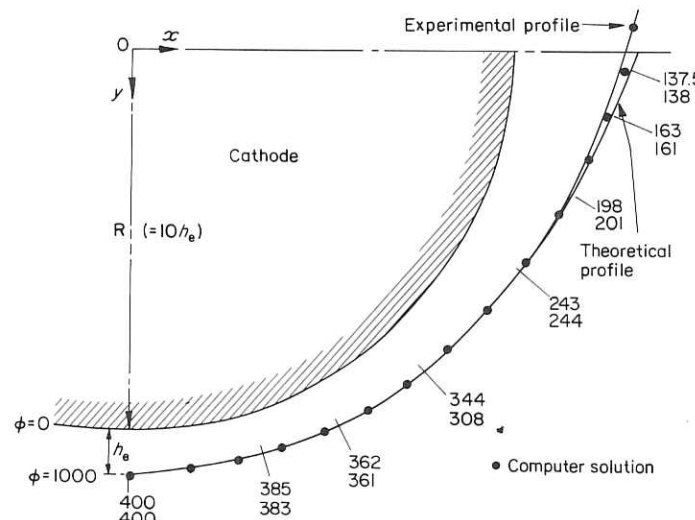


Fig. 7.17 Computer prediction and experimental anode shapes produced by semicircular cathode; Nimonic 90 anode; $h_e = 0.76 \text{ mm}$; $f = 0.02 \text{ mm/s}$; $I = 155 \text{ A}$; $V = 15 \text{ V}$; $Q = 1.6 \times 10^{-3} \text{ m}^3/\text{s}$; $\rho_e = 1.15 \text{ g/cm}^3$; $T = 26^\circ\text{C}$; pressure at inlet = 750 kN/m^2 (after Lawrence [6])

References

1. Fitz-Gerald, J. M., McGeough, J. A. and Marsh, L. M., *J. Inst. Math. and Applics.* (1969) 5, 409.
2. Collett, D. E., Hewson-Browne, R. C. and Windle, D. W., *J. Eng. Math.* (1970) 4, No. 1, 29.
3. Hewson-Browne, R. C., *J. Eng. Math.* (1971) 5, 233.
4. Tipton, H., Proc. Fifth Mach. Tool Des. Res. Conf., Birmingham, Pergamon Press (1964), 509.
5. Tipton, H., I.E.E. Conference on Electrical Methods of Machining and Forming, London, 1967. Conf. Public. No. 38, p. 48.
6. Lawrence, P., Ph.D. Thesis, Leicester University (submitted).
7. Kawafune, K., Mikoshiba, T. and Noto, K., *Ann. C.I.R.P.* (1968) 16, 345.
8. Tipton, H., in *Electrochemical Machining* (ed. A. E. DeBarr and D. A. Oliver), MacDonald, London (1968) Ch. 9.
9. Smith, G. D., *Numerical Solutions of Partial Differential Equations*, Oxford University Press, London (1965).
10. Tipton, H., in *Fundamentals of Electrochemical Machining* (ed. C. L. Faust), see Ref. 8, Ch. 4, p. 87.